Extraction of Features for Diagnosing Pneumoconiosis from Chest Radiographs Obtained with a CCD Scanner

Munehiro Nakamura[1], Koji Abe[2], Masahide Minami[3]
[1]Graduate School of Natural Science and Technology
Kanazawa UniversityKakuma
Kanazawa 920-1192
Japan
gm.nakamura@gmail.com

[2]Interdisciplinary Graduate School of Science and Engineering
Kinki University3-4-1
Kowakae, Higashi-Osaka
Osaka 577-8502, Japan
koji@info.kindai.ac.jp

[3]Graduate School of Medicine
The University of Tokyo7-3-1
Hongo, Bunkyo-ku
Tokyo 113-0033, Japan
maminami@dream.com

Journal of Digital Information Management

ABSTRACT: *This paper presents a computer-aided diagnosis for pneumoconiosis radiographs obtained with a common CCD scanner. Since the existing diagnosis systems for pneumoconiosis extract abnormalities of pneumoconiosis from images obtained with a special scanner which can appropriately apply for chest radiographs, it is difficult to apply the systems to images obtained with a CCD scanner due to unclear shadow and the systems are not practical for medical doctors due to high costs. In the unclear images, the abnormal levels of pneumoconiosis could depend on density distribution in each of intercostal and rib areas. Therefore, the proposed method measures the abnormalities by extracting characteristics of the distribution in the areas. Besides, using the abnormalities, the proposed method classifies the images into the three categories of pneumoconiosis. Experimental results of the classifications for 51 right-lung images including 6 pneumoconiosis images have shown that the proposed abnormalities are well extracted according to the standards of pneumoconiosis categories.*

Categories and Subject Descriptors
J 3 [Medical Information Systems]; I.4 [Image Processing and Computer Vision]: Segmentation

General Terms: Image classification, Medical image segmentation

Keywords: Computer-aided diagnosis, Pneumoconiosis, Chest radiographs, Medical image processing

Received: 28 July 2009, Revised 29 October 2009, Accepted 18 November 2009

1. Introduction

Pneumoconiosis is interstitial lung disease caused by inhaling fine particles (e.g., coal pneumoconiosis). In recent years, in addition to coal workers, dental technicians are suffered from the disease. However, since it is difficult for even experts on pneumoconiosis to diagnose pneumoconiosis, disagreement between medical doctors is often happened. Besides, educations of the diagnosis for inexperienced doctors have been conducted based on only experience of the experts. For the reasons, CAD (computer-aided diagnosis) systems for evaluating pneumoconiosis have been required as a second opinion for medical doctors.

CAD systems for pneumoconiosis have been reported since 1970s [1, 2, 3, 4, 5, 6, 7, 8, 9]. Their measurements of abnormalities for pneumoconiosis are broadly distinguished into two ways: the one measures the abnormalities extracting features obtained by texture analysis [1, 2, 3, 4, 5], another one extracts small round opacities from lung images and measures their size and number as well as the real diagnosis by doctors [6, 7, 8, 9]. All the systems have been proposed to images obtained with a special scanner such as a drum scanner or a film scanner. Therefore, in the case when the systems are applied in general hospitals, it is necessary to put the special scanner, or to order scanning chest radiographs to a printing company in spite of high cost. And, since the size of the special scanner for chest radiographs is not small, the scanner has no mobility. Hence, if there is a CAD system for pneumoconiosis which can be applied for images obtained with a common CCD scanner, the CAD system could be significantly managed in hospitals. However, since clearness of the shadow in lungs obtained with a CCD scanner is far worse than lungs obtained with the special scanners and the small round opacities are also not appeared clearly, the existing CAD systems cannot be applied to images obtained with a CCD scanner.

To enhance cost-performance and mobility of CAD for pneumoconiosis, this paper proposes a method for extracting abnormalities of pneumoconiosis from images obtained with a common CCD scanner. In addition, using the abnormalities, the proposed method diagnoses the images by classifying the images into the categories of pneumoconiosis defined in the Japanese Pneumoconiosis Law. The proposed CAD system is composed with a CCD scanner and a tablet PC. The abnormalities are measured by extracting characteristics of density distribution in each of intercostal and rib areas. The tablet PC is used to draw edges of ribs on the images, i.e., boundaries between intercostal and rib areas are input manually. And then, pneumoconiosis treated in this

paper means silicosis as well as all the existing literatures on CAD for pneumoconiosis.

In Section 2, we introduce the pneumoconiosis categorization defined in Japanese Pneumoconiosis Law. In Section 3, we examine difference of shadow clearness in lungs between images obtained with a drum scanner and a CCD scanner. In Section 4, we propose a method for extracting abnormalities of pneumoconiosis. And then, in Section 5, we confirm performance of the proposed method from experimental results obtained by classifications of the images according to the pneumoconiosis categorization.

2. Pneumoconiosis Categorization

The severity of pneumoconiosis is indicated by profusion of small round opacities, where categories 0 – 4 have been established. Normal radiographs belong to category 0, where the opacities are not observed visually. And, abnormal ones belong to category 1, 2, 3, or 4, where the most serious level is category 4 and the opacities are observed most in category 4. Although medical doctors diagnose pneumoconiosis according to the criteria and the standard pneumoconiosis radiographs prepared to every category, their own experience much depends on the diagnosis because they need to observe subtle difference between a target and the standard radiographs visually in the diagnosis.

The criteria are defined in the Japanese Pneumoconiosis Law in accordance with criteria of pneumoconiosis in ILO (The International Labour Organization) and the Japanese standard pneumoconiosis radiographs have been provided by the Ministry of Health, Labor and Welfare, Japan.

3. Visual Difference between Pneumoconiosis Radiographs Obtained with CCD Scanner and Drum Scanner

Figure 1 shows a chest radiograph image obtained with a drum scanner and a histogram of pixel values in the part shown in the image. On the other hands, Figure 2 shows a chest image obtained with a CCD scanner and a histogram of pixel values in the part shown in the image, where the chest radiograph for the image is the same one shown in Figure 1 and the location of the part is also the same as Figure 1. From both of the histograms, we can see their distributions are quite different. Thus, since CCD scanner can not accurately reproduce permeable films such as radiographs, the visibility of lung in the image obtained with CCD scanner is considerably lower than drum scanner. For the reason, it is suggested that the existing systems [6, 7, 8, 9] can not extract small round opacities from chest radiograph images obtained with CCD

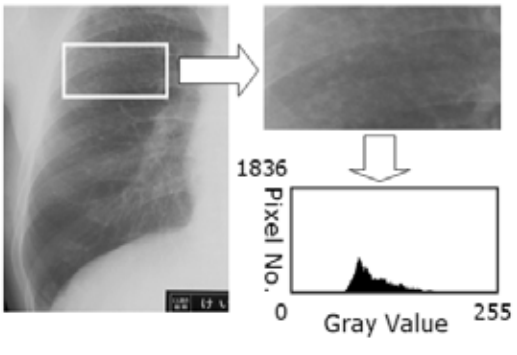

Figure 1. A chest radiographs image obtained with drum scanner and the histogram of pixel values in the part shown in the image

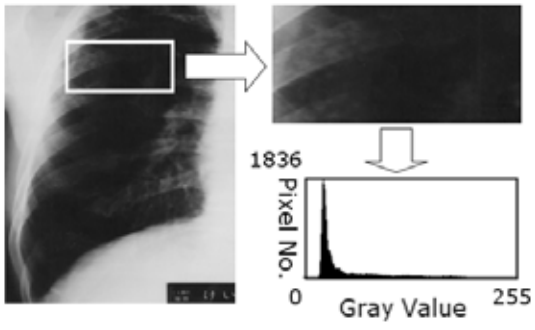

Figure 2. A chest radiographs image obtained with CCD scanner and the histogram of pixel values in the same area as the part in Figure 1 (The radiograph is the same as Figure 1)

scanner. Similarly, since the texture analysis is significantly affected by the image quality, texture analysis [1, 2, 3, 4, 5] could not effectively extract features from the images. Therefore, it would be necessary to propose a novel method to design a CAD for pneumoconiosis in radiograph images obtained with CCD scanner.

4. Proposed Method

4.1 Determination of Target Areas for Extracting the Abnormalities

Although most of the small round opacities have been disappeared in chest radiograph images obtained with CCD scanner, we could perceive characteristics of pneumoconiosis radiographs in each category. In images of category 0, opacities are not found. In images of category 1, a few opacities are observed around rib edges. And, in images of category 2, numerous opacities are observed in rib areas. Besides, in images of category 3, the opacities are much observed than category 2 in both of intercostal and rib areas. As other characteristics of pneumoconiosis images obtained with CCD scanner by the observation: 1) density in outside of the lung area is higher and inside of the lung area is lower than drum scanner, and, 2) the opacities tend to appear around rib edges since the contrast is extremely high near the edges. Thus, for the sake of a CAD for pneumoconiosis obtained with CCD scanner, it could be effective to obtain boundaries between intercostal and rib areas and extract characteristics of pneumoconiosis from the areas. In this paper, since images of category 4 can be clearly distinguished at a glance, we deal with only categories 0 – 3.

In the proposed CAD system, the diagnosis is conducted with a CCD scanner and a tablet PC, where the tablet PC is used to draw rib edges manually. First, the user draws the 10 rib edges on the images obtained with the CCD scanner with the tablet PC and images where the edges were drawn are prepared. Next, using the images, the proposed abnormalities of pneumoconiosis are measured based on the density distribution in each of intercostal and rib areas. Finally, using the abnormalities, the pneumoconiosis categorization is performed.

4.2 Preprocessing

The CCD scanner converts chest radiographs into digital images with 8 bits of gray level. And since the whole density of the images is very low an d the range of their gray level is not maximally used as shown in Figure 2, a normalization such as moving normalization [9] would be needed. However, the moving normalization could emphasize harmful parts such as vessel's shadows. Hence, the normal normalization is applied

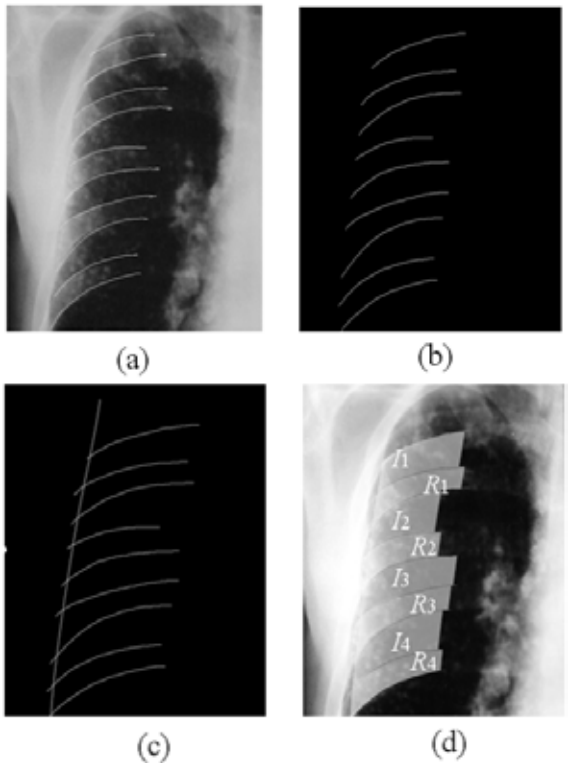

Figure 3. Process for obtaining target areas for extracting abnormalities of pneumoconiosis

to the images. After then, to reduce noises in the images, the selective local averaging is repeated twice.

4.3 Determination of Target Areas for Extracting the Abnormalities

In order to extract characteristics of pneumoconiosis from the density distribution in the lung area, considering characteristics of lung images obtained with CCD scanner shown above, it is necessary to extract intercostal and rib areas separately. Regarding the extraction, an automatic segmentation of ribs in chest radiographs was reported [10]. However, this method would not be appropriate for the extraction because the segmented ribs would include unnecessary parts for the extraction such as heart shadow, and the method has not been examined as an application for images obtained with CCD scanner.

In the proposed CAD, the areas are extracted by drawing boundaries between intercostal and rib areas manually using the tablet PC as shown in Figure 3(a). Concretely, the image is displayed on the tablet PC and the user draws 10 rib edges on the image with the tablet PC according to a rule for drawing we prepared. Pixel values of the drawn rib edges are quantized as 255 (white) and the other parts are quantized between 0 and 254 in advance. Then, only the edges are extracted by the labeling for pixel value of 255 as shown in Figure 3(b). Next, a curve is obtained by B-spline functions with the ten coordinates located at the most outside of the rib edges as shown in Figure 3(c). It means the curve is obtained along the outside of a lung. And, shifting the curve to the inside of the lung horizontally, both of side boundaries in the rib and intercostal areas are obtained as shown in Figure 3(d). Figure 3(d) shows target areas for extracting abnormalities of pneumoconiosis, where R1, R2, R3, and R4 are the rib areas, and I1, I2, I3, and I4 are the intercostal areas. Among the areas extracted by the 10 edges, the most upper area is not used (as R0) because the shadow of the collarbone appears in the area depending on participants.

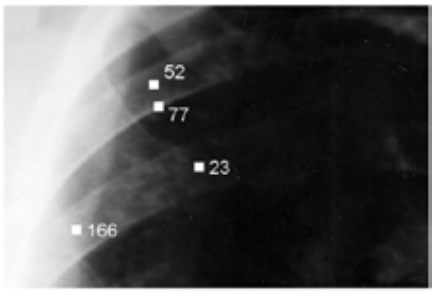

Figure 4. Pixels values at some locations in a pneumoconiosis radiograph (category 2) obtained with CCD scanner

4.4 Extraction of Abnormalities

Resulting from examinations of density distribution in the target areas, we obtained the following characteristics: 1) the lung field keeps bright only at the outside, where we can distinguish pneumoconiosis from normal chests, 2) the density of rib edges is specially high and pixels around the edges have lower values as distance between the pixels and the edges is much, and 3) the opacities are appeared randomly. The four pixel values shown in Figure 4 represent these characteristics. Considering the characteristics, the abnormalities of pneumoconiosis are extracted from each of the rib and intercostal areas as below.

Regarding the curve shown in Figure 3(c) as the initial scanning line for all the target areas, the value 1 is put into the scanning number k, which increases 1 whenever the curve once shifts 1 pixel to the inside of the lung. And then, when the central pixel of the curve segment between two edges which determine a rib area R is regarded as c_1, the abnormality of pneumoconiosis in the first scanning is defined as

$$abn(R[1]) = \frac{1}{diamtr[1]} \sum_{j=1}^{diamtr[1]} |u[1,j] - l[1,j]|^2 \quad (1)$$

where $diamtr[1]$ is the number of pixels which form the curve segment between c_1 and one of the intersections at which the curve and the edges cross each other (i.e., $diamtr[1]$ is half of the length of the curve segment); $u[1,j]$ and $l[1,j]$ are pixel values of the j th scanning spots when a scanning is conducted from c_1 to each of the upper intersection and the lower one along the curve. $abn(R[1])$ represents mean of $|u[1, j] - l[1, j]|^2$ in the first scan for the rib area. By shifting the curve horizontally toward the inside of the lung by 1 pixel until the another side boundary of the rib area, the abnormality in a rib area R_m (m = 1, 2, 3, or 4) is given by

$$Abn(R_m) = \left[\frac{1}{length_m} \sum_{k=1}^{length_m} abn(R[k]) \right]^{1/2} \left[\frac{1}{length_m} \sum_{k=1}^{length_m} \left\{ \frac{1}{diamtr[k]} \sum_{j=1}^{diamtr[k]} |u[k,j] - l[k,j]|^2 \right\} \right]^{1/2} \quad (2)$$

where $length_m$ is the number of the shifts in R_m, $diamtr[k]$ is the number of pixels which form the curve segment between c_k and one of the intersections at which the kth scanning curve and the edges cross each other, and then, $u[k, j]$, and $l[k, j]$ are pixel values of the jth scanning spots when the kth scanning is conducted from c_k to each of the upper intersection and the lower one along the k th scanning curve, respectively. $Abn(R_m)$ represents the mean of *abn* obtained from all the scanning curves in R_m. Since the number of the rib areas is 4, the abnormality obtained from all the rib areas Abn_R is defined as

$$Abn_R = \left[\frac{1}{L_R}\sum_{m=1}^{4}\sum_{k=1}^{length_m}\left\{\frac{1}{diamtr[m,k]}\sum_{j=1}^{diamtr[k]}|u[m,k,j]-l[m,k,j]|^2\right\}\right]^{1/2} \quad (3)$$

where $diamtr[m, k]$, $u[m, k, j]$, and $l[m, k, j]$ are $diamtr[k]$, $u[k, j]$, and $l[k, j]$ in R_m, respectively, and

$$L_R = \sum_{m=1}^{4} length_m \quad (4)$$

Similarly, the abnormality in one of the intercostal areas I_m is given by

$$Abn(I_m) = \left[\frac{1}{leng_m}\sum_{k=1}^{leng_m}\left\{\frac{1}{inter[k]}\sum_{j=1}^{inter[k]}|v[k,j]-w[k,j]|^2\right\}\right]^{1/2} \quad (5)$$

where $leng_m$ is the number of the shifts in I_m, $inter[k]$ is the number of pixels which form the curve segment between C_k and one of the intersections at which the kth scanning curve and the edges cross each other, and then, $v[k, j]$, and $w[k, j]$ are pixel values of the jth scanning spots when the kth scanning is conducted from C_k to each of the upper intersection and the lower one along the kth scanning curve, respectively. C_k is the central point of the curve segment between two edges which determine I_m. Besides, the abnormality obtained from all the intercostal areas Abn_I is defined as

$$Abn_I = \left[\frac{1}{L_I}\sum_{m=1}^{4}\sum_{k=1}^{leng_m}\left\{\frac{1}{inter[m,k]}\sum_{j=1}^{inter[m,k]}\left|v[m,k,j]-w[m,k,j]\right|^2\right\}\right]^{1/2} \quad (6)$$

where $inter[m, k]$, $v[m, k, j]$, and $w[m, k, j]$ are $inter[k]$, $v[k, j]$, and $w[k, j]$ in I_m, respectively, and

$$L_I = \sum_{m=1}^{4} leng_m \quad (7)$$

Thus, the abnormalities of pneumoconiosis are extracted from a lung in a chest radiograph as Abn_R and Abn_I.

5. Experimental Results

We applied the proposed abnormalities to 51 chest radiographs (35cm×35cm). The radiographs were scanned with a CCD scanner (EPSON GT-X750) and only the right lung in every of the radiographs was obtained (resolution: 400dpi, gray level: 8 bits). In the radiographs, the number of images which are in category 0 is 45, the number in category 1 is 4, the number in category 2 is 1, and the number in category 3 is 1. The 6 pneumoconiosis radiographs are the standard pneumoconiosis radiographs provided by the Ministry of Health, Labor and Welfare in Japan. To obtain the target areas, a medical doctor drew 10 rib edges in all of the 51 lung images with a tablet PC (HP Compaq TC400).

Table 1 shows the mean value of the two abnormalities extracted from the images in each category. And then, Table 2 shows the standard deviation of the abnormalities in categories 0 and 1. As shown in two of the tables, we can confirm both of the abnormalities have been increased gradually according to increase of the category level.

Category level	Abn_R	Abn_I
0(45 images)	7.9	9.6
1(4 images)	18.4	17.2
2(1 image)	17.9	13.9
3(1 image)	20.6	18.4

Table 1. The mean value of the abnormalities extracted from the 51 data in each category

Category level	Abn_R	Abn_I
0 (45 images)	2.4	3.5
1(4 images)	1.7	3.7

Table 2. The standard deviation of the abnormalities extracted from the 49 data in categories 0 and 1

Next, to examine performances of the two abnormalities as features for an automated categorization of pneumoconiosis categories, random trees (RT), a neural network (NN), and a supports vector machine (SVM) categorized the images into the pneumoconiosis categories regarding the abnormalities as two features of pneumoconiosis, respectively. In all the categorizations, training set and test set were chosen by cross validation [11]. In fact, every categorization was conducted as the following procedure:

1. Choose one from all the data as test data, and use the other data as training set.
2. Conduct the categorization for discriminating the test data between category 0 and the other categories.
3. Conduct the categorization for discriminating the test data between category 0 or 1 and category 2 or 3.
4. Conduct the procedure from (1) to (3) to every data changing the test data.
5. Repeat the procedure from (1) to (4) 100 times.

Figure 5 shows a trial of the cross validation.

Thus, the categorizations twice discriminated the images between images of category 0 and the others, and then between category 0 – 1 (0 or 1) and category 2 – 3 (2 or 3). In the 100 trials, every of the categorizations does not always output the same result. In RT, the values of the optimal segmentation are randomly selected in every tree, and, in NN and SVM, the discriminant functions differ in every trial since perceptron selects training data randomly.

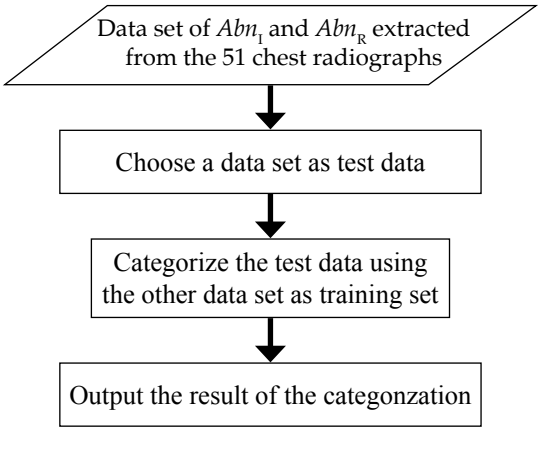

Figure 5. A flow of a trial in the cross validation used in the experiments

Table 3 and Table 4 show the means and standard deviations (STD) of correct ratios in the 100 trials by each categorization between category 0 and the others, and between category 0 – 1 and category 2 – 3 respectively. Table 3 represents the mean of recognition ratio for images in category 0 is more than 90% in every categorization. Similarly, Table 4 represents the mean for images in category 0 – 1 is more than 90% in every categorization. According to the results shown in the two tables, in the categorizations of pneumoconiosis using the proposed abnormalities, the abnormalities are most effective in the categorizations by SVM.

Category	**0**		**1-3**	
	Mean	**STD**	**Mean**	**STD**
RT	97.5%	1.3	38.7%	12.8
NN	97.3%	1.1	48.3%	13.2
SVM	98.9%	1.1	100.0%	0.0

Table 3. Mean and standard deviation of correct ratios in the categorizations (Discrimination between category 0 and the other categories)

Category	**0**		**1-3**	
	Mean	**STD**	**Mean**	**STD**
RT	98.1%	1.3	74.5%	29.6
NN	95.1%	2.0	100.0%	0.0
SVM	98.9%	1.1	100.0%	0.0

Table 4. Mean and standard deviation of correct ratios in the categorizations (Discrimination between category 0 or 1 and category 2 or 3)

Figure 6 (left) shows an image in category 1 which was discriminated into category 2–3 as an error (error case) and Figure 6 (right) shows the image in category 3. Table 5 shows the abnormalities Abn (refer to Eqs. (2) and (5)) of every rib and every intercostal area in the two images and the standard deviations obtained from all of abn (refer to Eqs. (1), (2), and (5)) in each of the target areas in the two images. In Figure 6, we can observe that the left image of error case does not show the opacities so much comparing with the right image. However, most of the abnormalities for error case are higher than image of category 3. Figure 7 (right) shows the target areas of I_4 and R_4 in the error case (left). Figure 7 (left) is the image of error case attaching edges drawn by the participant. The abnormalities in the I_4 and R_4 and their standard deviations are especially high, and we can observe the drawn curves are off the true edges. Besides, other ribs appear in the target areas like a gradation and the density distribution in the areas vary widely. Considering the calculation way of the proposed

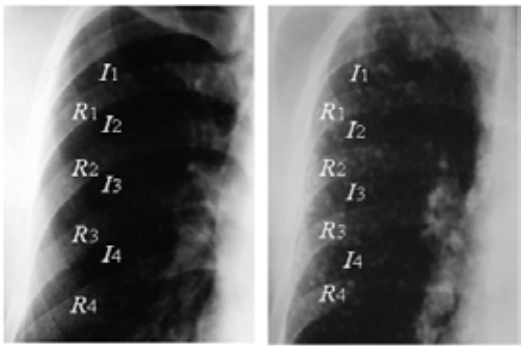

Figure 6. The error case in the experiments (left) and the image in category 3 (right)

$Abn(x)$								
x	R_1	R_2	R_3	R_4	I_1	I_2	T_3	I_4
category 3	14.2	13.9	19.3	20.4	26.7	19.4	19.0	19.4
error case	14.9	22.0	23.8	23.6	13.0	19.6	11.0	28.4
standard deviation for all of abn in area x								
x	R_1	R_2	R_3	R_4	I_1	I_2	I_3	I_4
category 3	41.6	25.1	55.5	79.9	95.5	72.8	69.7	42.4
error case	39.6	89.2	191.7	177.1	31.1	57.1	17.8	139.1

Table 5. Parameters $Abn(x)$ in the abnormalities for the images of categorization failure and the standard deviation for all of abn in the target area x

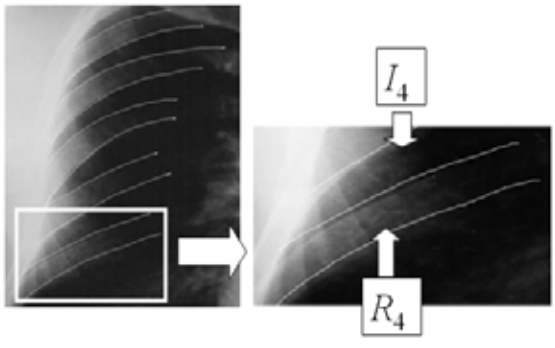

Figure 7. The target areas of R_4 and I_4 and edges drawn by the participant in the image of error case

abnormalities, the abnormalities in areas such as this could be calculated higher than real situation.

For the reason, to extract the abnormalities more accurately, i.e., to draw the edges more accurately, it would be necessary to design a manual for drawing rib edges or to prepare an interface for drawing the edges easy and exactly.

6. Conclusions

To enhance cost-performance and mobility in CAD systems for pneumoconiosis, this paper has presented a method for extracting abnormalities of pneumoconiosis from chest radiographs obtained with a CCD scanner. The abnormalities are extracted from each of the ribs and intercostal areas by examining density distribution in the areas, and the edges are manually drawn with a tablet PC. Then, regarding the abnormalities as features of the categorization of pneumoconiosis, this paper has examined performance of the abnormalities by three automated categorizations. Experimental results of the categorizations have shown that the proposed abnormalities are most effective in the categorization by SVM among the three ways.

Considering the cases of categorization failure, we would like to design a manual or prepare an interface for drawing the edges more accurately as a future work. Besides, we need to examine performance of the proposed method to pneumoconiosis radiographs provided by the ILO as well.

References

[1] Kruger, R. P., Thompson, W. B. (1974). Computer diagnosis of pneumoconiosis. *Trans. on Systems. Man and Cybernetics*, SMC-4 (1) 40–49.

[2] Huang, H., Ledley, R., Rotola, L. (1975). A texture analysis method in classification of coal workers pneumoconiosis. *Comput. Biol. Med*, 5, 53–67.

[3] Stark, H., Lee, D. (1976). An optical-digital approach to the pattern recognition of coalworkers 'pneumoconiosis. *IEEE Trans. Syst., Man Cybern*, SMC-6, 788–793.

[4] Jagoe, J. (1979). Gradient pattern coding–an application to the measurement of pneumoconiosis in chest x-rays. *Comput. Biomed. Res*, 12, 1–15.

[5] Ohishi, K., Kobatake, H., Miyauchi, J. (1987). Automatic diagnosis of pneumoconiosis by texture analysis of chest x-ray images, *In: Proc IEEE Int. Conf. Acoust. Speech Signal Process,* 610 – 613.

[6] Li, C., Savol, A. M., Hoy, R. J., (1980). Computer-aided recognition of small rounded pneumoconiosis opacities in chest x-rays. *IEEE Trans Pattern Anal. Mach. Intell*, 2 (5) 479–482.

[7] Hasegawa, J., Xuan, C., Toriwaki, J. (1988). Quantitative diagnosis of pneumoconiosis based on recognition of small rounded opacities in chest x-ray images. *In: Proc. the 9th ICPR*, 462–464.

[8] Wei, J., Kobatake, H. (1999). Detection of rounded opacities on chest radiographs using convergence index filter. *In: Proc. ICIAP*, 757–761.

[9] Kouda,T., Kondo, H. (2001). Computer-aided diagnosis for pneumoconiosis using neural network. *Biomed. Soft Comput. Hum. Sci*, 7 (1) 13–18.

[10] Loog, M., Van Ginneken, B. (2006). Segmentation of the posterior ribs in chest radiographs using iterated contextual pixel classification. *IEEE Trans. on Medical Imaging*, 25 (5) 602–611.

[11] Mosteller, F. (1948). A k-sample slippage test for an extreme population. *The Annals of Mathematical Statistics*, 19 (1) 58–65.

Authors Biographies

Munehiro Nakamura received his B.E. and M.E. from Kinki University, Japan, in 2008 and 2010, respectively. Currently, he is a Ph.D. candidate in Graduate School of Natural Science and Technology, Kanazawa University, Japan. His research interests include medical image processing and pattern recognition. He is a member of IEICE (Japan).

Koji Abe received his B.S. and M.S. degrees from Kogakuin University, Japan, in 1996 and 1998, respectively. And, he received his Ph.D. degree in Engineering from Kanazawa University, Japan, in 2001. After that, he affiliated in the Institute for Image Data Research, University of Northumbria at Newcastle, UK, as an honorary research fellow in 2002. He was an assistant professor in Kanazawa Institute of Technology, Japan, in 2003. Currently, he is an associate professor in the Dept. of Informatics, School of Science and Engineering, Kinki University, Japan. His research interests include pattern recognition, medical image processing, CBIR, multimedia database, and artificial intelligence. He is a member of IEEE, IEICE (Japan), IPSJ (Japan), and IEEJ (Japan).

Masahide Minami received his M.D. degree from University of Tsukuba, Japan, in 1989. And, he received his Ph.D. from Kanazawa University, Japan, in 1990. He affiliated in Dept. of 2nd Surgery, Kanazawa University in 1990 and Kanazawa Social Insurance Hospital in 1996, respectively. Besides, he received his LL.M. degree from Waseda University in 2002. Currently, he is the Head Physician in Health Control Department, Komatsu Ltd. Also, he is currently a Ph.D. candidate in Grad. Sch. of Medicine, the University of Tokyo. His research interests include cancer diagnostics and treatment, public health, and industrial hygiene. He is a member of Japan Surgical Society, Japanese Cancer Association, Japan Society for Occupational Health, and Japanese Society of Public Health.